BIBECHANA
ISSN 2091-0762 (Print), 2382-5340 (Online)
Journal homepage: http://nepjol.info/index.php/BIBECHANA
Publisher: Department of Physics, Mahendra Morang A.M. Campus, TU, Biratnagar, Nepal

Study of *aerosol* optical properties at different tourist places of Nepal

Rejeena Jha[1], Binod Adhikari[1*], Dharmendra Kumar Singh[2]
[1]Department of Physics, St. Xavier's College, Maitighar, Kathmandu, Nepal
[2]French National Center for Scientific Research (CNRS) /IRCELyon, Villeurbanne-69100, France
[*]E-mail address: binod.adhikari@sxc.edu.np

Article Information:
Received: July 6, 2020
Accepted: August 26, 2020

Keywords:
Aerosol optical depth (AOD)
Angstrom exponent
Cloud condensation
Cross-correlation coefficient

ABSTRACT
The comparative study of aerosol optical properties at different tourist places of Nepal has been performed. Langtang BC, Lumbini, Pokhara, Kathmandu-bode, EVK2-CNR, Jomsom and Kyanjin_Gompa were the places chosen for observation. We have analyzed the monthly and seasonal variation of aerosol optical properties for a different year of the above-mentioned places. AOD was found to be maximum in spring due to vegetation fire and land clearing for crop cultivation and, then in winter due to biomass burning, heating needs, pollution from bricks kilns, factories, and vehicles that contribute to winter haze. It consequently decreases in summer and was found to be minimum in autumn as summer constituent both dry and wet days and autumn starts with the ending of monsoon. But it was quite different in the case of Pokhara where it was minimum in summer than in autumn as Pokhara is the only city where maximum rainfall occurs in summer. We have also studied the relation between AOD and corresponding wavelength. It was acclaimed that the AOD of shorter wavelength is more than the longer one which is because of angstrom exponent. The relation between AOD and precipitated water has been observed and noticed one to one correspondence except July and August. The cross-correlation between these two factors found to be very high indicating a time lag of approximately 2 months with the presence of aerosol on cloud condensation nuclei (CCN).

DOI: https://doi.org/10.3126/bibechana.v18i1.29906

1. Introduction

Nanomaterials are considered as intermediate The degrading air quality, particularly in population-dense areas, is associated with high aerosol levels (both anthropogenic and natural [1]. System of solid or liquid particles suspended by a mixture of gases [2], called aerosols, cover a wide spectrum dominated by dust, sulfate, carbon, sea salt, or mixtures of these particles [3] It is considered one

of the important factors in the current prediction of global climate change but associated with large uncertainties. It is a key component to study atmospheric physics such as radiative transfer of light waves in atmosphere and precipitation[4]. They directly affect the earth's solar radiation budget by scattering and absorbing solar and thermal radiation[5]. On the other hand, aerosols can also act as cloud condensation nuclei (CCN), impacting cloud cover, cloud properties, and precipitation, ultimately influencing the hydrological cycle [6]. An increase in aerosol concentration generally results in more numerous, but smaller, droplets for a given liquid water content, which ends up in a rise of the cloud albedo, known as the first indirect effect. Further, a decrease in cloud droplet size delays and reduces precipitation processes, which is referred to as the second indirect effect. However, numerous feedbacks and interactions with the ice phase and other aspects of cloud dynamics make it difficult to tease out exactly how cloud microphysical changes due to aerosol changes affect the radiative balance, precipitation, and dynamics systematically and quantitatively [7].

Moreover, Aerosol plays a significant role in reducing visibility and implication in human health hazard because sub-micron aerosols can irritate the respiratory system [8]. Even Epidemiological and toxicological studies have shown associations between aerosols and adverse health effects [9]. The Tibetan Plateau (TP), the largest and highest plateau on earth, usually acts as a receptor of natural and anthropogenic aerosols from the surrounding regions, and its environment is highly sensitive to climate change and human activities [6]. The Himalaya Mountain located along the southern edge of the TP acts as a natural barrier for the transport of atmospheric aerosols [6]. Aerosol Optical Depth (AOD), defined as the ratio of solar radiation absorbed to the ratio of total solar radiation transmitted, determines how much direct sunlight is prevented from reaching the ground by the aerosol particles[10]. This work mainly focuses on the understanding of AOD behavior concerning wavelength and precipitated water on monthly variation and also describes the seasonal variation of AOD of different stations.

Datasets

In this section, we have discussed the site's location, sources of data collection, and methodology which have been implemented on this work. We have observed AOD from Langtang BC, Lumbini, Pokhara, Kathmandu-bode, EVK2-CNR, Jomsom, and Kyanjin_Gompa. Langtang BC, EVK2-CNR, and Jomsom are in the Himalayan region of Nepal, Pokhara. Kathmandu-bode lies in the Hilly region and Lumbini is in the Terai region of Nepal. These places are considered as the major tourist places where Lumbini, Kathmandu-bode, and Pokhara are densely populated cities, while the population of Langtang BC, EVK2-CNR, and Jomsom are comparatively slim. Pokhara is a lower-elevation suburban site with much higher aerosol load due to both the influence of local anthropogenic activities and its proximity to the Indo-Gangetic Plains [6] Over 125 brick kilns are in Kathmandu-Bode, which contribute significantly to atmospheric aerosols, particularly during winters. In the Himalayan regions, people hugely rely on the traditional way of cooking by burning biomass (e.g. cow-dung, wood, fuel), which releases a large amount of aerosol in the atmosphere. The detailed description of the sites is given below in the table [11].The satellite data are considered as one of the main sources to describe the nature of aerosol optical properties. The data for the research was extracted from the AERONET site and this paper has used 2.0 version of data which is quality assured. AERONET uses ASCII text format for data transfer to improve data transfer between systems. The Aerosol Robotic Network is a ground-based network of standardized Cimel Sun and sky scanning radiometers measuring AOD at multiple wavelengths from 340 to 1640 nm and retrieving other columnar optically effective aerosol properties [3] like volume, size distribution,

aerosol optical depth (AOD), total optical depth (TOD), etc. The development of the Aerosol Robotic Network (AERONET) for monitoring aerosol optical depth provides measurements of natural and anthropogenic aerosol loading, which is important in many local and regional studies as well as global change research investigation [12]. AERONET is the ground-based sun-photometer network with over 400 stations globally. The AERONET AOD is derived from direct beams of solar measurements. This study is dedicated to presenting a trend analysis at selected stations. The monthly mean as well as daily averages of AOD are available at AERONET. AERONET has been providing high-quality retrievals of aerosol optical properties from the surface at worldwide locations for quite a decade. Many sites have continuous and consistent records for over 10 years, which enables the investigation of long-term trends in aerosol properties at these locations:

	Sites coordinates and elevation	**Site description**
Langtang BC	Latitude: 28.21443° North Longitude: 85.60978° East Elevation: 4901.0 Meters	The Instrument located in Langtang valley near Yala glacier in the fenced area of the ICMOD met station[13].
Lumbini	Latitude: 27.49000° North Longitude: 83.28000° East Elevation: 110.0 Meters	The site is in the Southern plain of Nepal, which is a part of the Indo-Gangetic plain [14].
Pokhara	Latitude: 28.18664° North Longitude: 83.97518° East Elevation: 800.0 Meters	The instrument is located on the roof of Shangrila Village Resort, on the south-western outskirts of Pokhara City, Nepal[15].
Kathmandu-bode	Latitude: 27.68000° North Longitude: 85.39000° East Elevation: 1297.0 Meters	The site is in agricultural-residential setting downwind of the Kathmandu city, near the village of Bode, Bhaktapur District[16].
EVK2-CNR	Latitude: 27.95775° North Longitude: 86.81494° East Elevation: 5079.0 Meters	The Cimel sun photometer is operated at the Nepal Climate Observatory at Pyramid (NCO-P), at 5079 m asl, in the Khumbu valley, Nepal, close to the Pyramid International Laboratory[17].
Jomsom	Latitude: 28.77821° North Longitude: 83.71420° East Elevation: 2825.0 Meters	On the roof of a single-story laboratory building at the southern corner of a plateau sticking into the wind blowing up the Kali Gandaki Valley[18].
Kyanjin_Gompa	Latitude: 28.21126° North Longitude: 85.56630° East Elevation: 3862.0 Meters	Instrument located in Langtang valley near Kyanjin_Gompa village in the fenced area of the ICMOD met station[19].

2. Methodology

The cross-correlation between AOD and precipitable water has been observed. Cross-correlation: the measurement that tracks the movements of two variables or sets of knowledge relative to every other[20] and most importantly it is use to find the lag/lead/time of maximum correlation. Here the cross-correlation between precipitated water and AOD at 1020nm, 870nm, and 675nm has been observed. The term cross-

correlations are used for referring to the correlations between the entries of two random vectors X and Y, while the correlation of a random vector X is considered to be correlations between the entries of X itself, those forming the correlation of X [21]. The definition of correlation always includes a standardizing factor in such a way that correlations have values between −1 and +1 [22]. The period for this study was from Jan 1st to Dec 31st, 2018 of Langtang BC, Lumbini and Pokhara, also, Jan 1st to Dec 31st, 2013 of Kathmandu-bode and the same period of EVK2-CNR and Jomsom in the year 2012.

A contour plot is a graphical form to depict a 3-dimensional surface by plotting constant z slices, called contours, on a 2-dimensional configuration. That is, given a value for z, lines are drawn for connecting the (x y) coordinates where that z value occurs [23]. The contour has been used to observe the seasonal variation of AOD in the above stations. Four seasons are defined as spring (March-May), summer (June-August), autumn (September-November), and winter (December-February) to investigate the seasonal variation of aerosol optical properties of various tourist places of Nepal.

3. Results and Discussion

In this section, we have discussed the result of monthly and seasonal variation of AOD to various wavelengths and precipitated water.

Relation of AOD with wavelengths and precipitated water

First, three panels of Figure 1 to Figure 6 show the variation of AOD to three wavelengths, 1020nm, 870nm, and 675 nm, respectively. The AOD of shorter wavelength is greater than the longer wavelength and vice-versa. The Angstrom exponent of AOD of shorter wavelength is greater than the longer one as the wavelength dependence of aerosols is strongly influenced by their chemical and size composition as a result show by[24]. The comparison between the first three panels of AOD at three different wavelengths with the precipitated water (figure 1 to figure 6) shows similar trends except in July and August (i.e., July and august mainly includes wet days of months). For a better understanding, we have implemented the cross-correlation analysis between them. Figure 7 to figure 12 represent the cross-correlation between precipitated water and AOD at wavelengths of 1020nm, 870nm, and 675nm from different stations. In the figure, the blue curve represents the cross-correlation between precipitated water and AOD at 1020nm, the red curve represents the cross-correlation precipitated water and AOD at 870nm and the green curve shows the cross-correlation of precipitated water and AOD at 675nm. In each figure, cross-correlation coefficients are on the y-axis, and time is kept at the x-axis. The cross-correlation coefficient of AOD of wavelengths 1020nm, 870nm, 675nm and precipitated water was found to be very high i.e., ~0.9 of Langtang BC in year 2018A.D, ~0.87 of Lumbini in year 2018A.D, ~0.88 of Pokhara in year 2018A.D, ~0.9 of Kathmandu-Bode in year 2013A.D, ~0.93 of EVK2-CNR in year 2012A.D, ~0.95 of Jomsom in year 2012A.D. These results show that the AOD and precipitated water are highly correlated on all stations. As much of the removal of atmospheric aerosols occurs in the vicinity of large weather systems and high-altitude jet streams, where the stratosphere and the lower atmosphere become intertwined and exchange air with each other, mentioned by [25]. In such regions, many pollutant gases within the troposphere are often injected within the stratosphere, affecting the chemistry of the stratosphere. Likewise, in such regions, the ozone within the stratosphere is brought right down to the lower atmosphere where it reacts with the pollutant rich air, possibly forming new kinds of pollution aerosols. So, for the removal of a large amount of aerosol there must occur enduring and a battery of natural calamities similar as the result of [26].

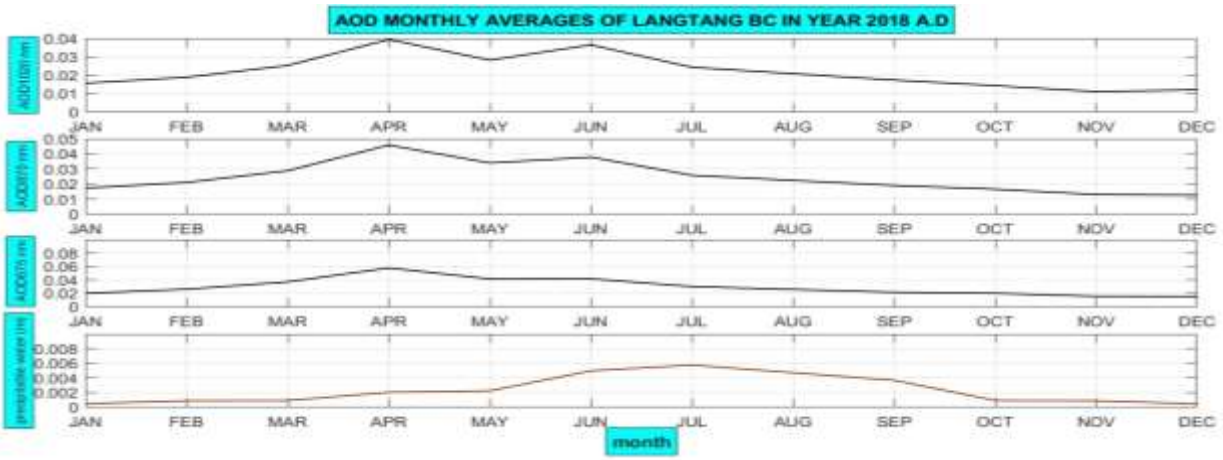

Fig. 1: The first three panel shows the variation of AOD with respect to three different wavelengths i.e. 1020nm, 870nm and 675nm respectively and, the fourth panel shows the variation of AOD to precipitated water of Langtang BC in the Year 2018 A.D.

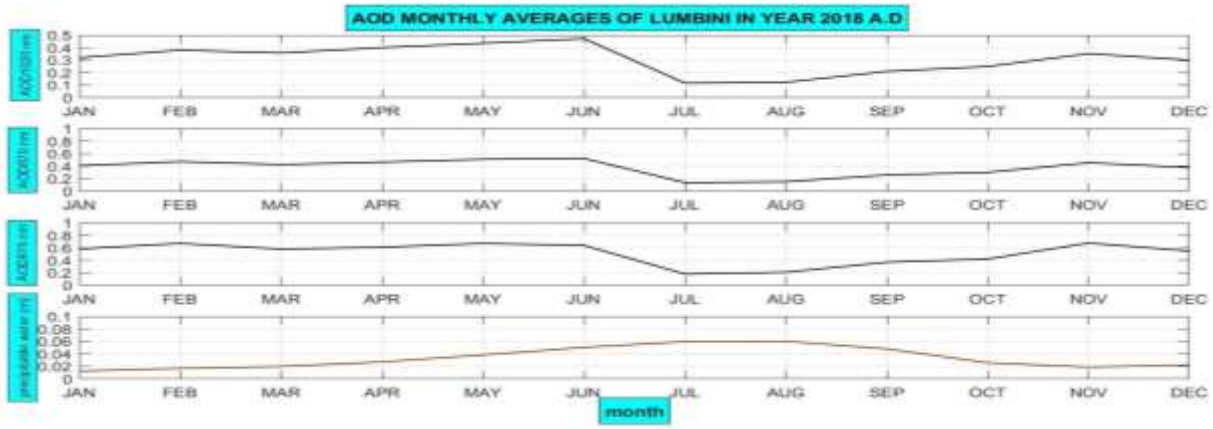

Fig. 2: The first three panel shows the variation of AOD with respect to three different wavelength i.e. 1020nm, 870nm and 675nm respectively and, the fourth panel shows the variation of AOD to precipitated water of Lumbini in Year 2018 A.D.

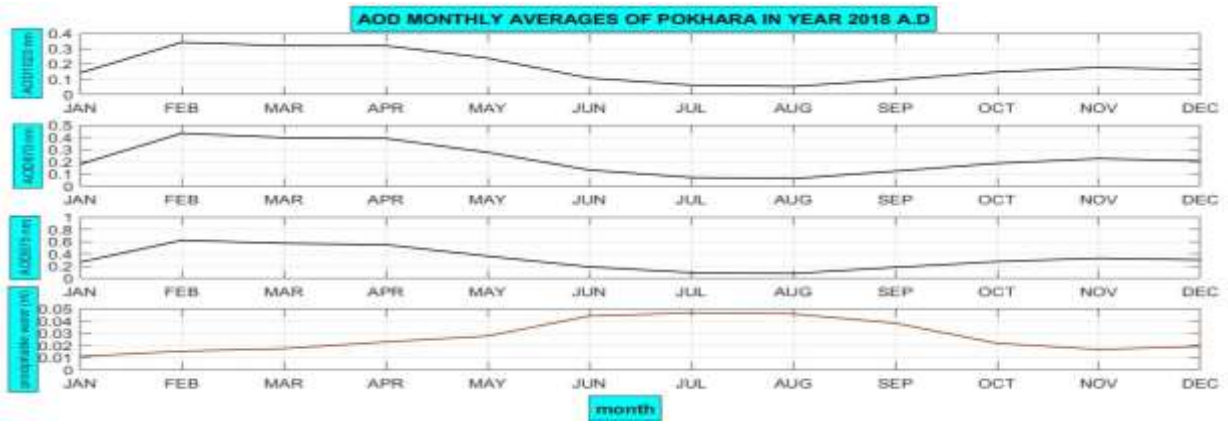

Fig. 3: The first three panel shows the variation of AOD with respect to three different wavelength i.e. 1020nm, 870nm and 675nm respectively and, the fourth panel shows the variation of AOD to precipitated water of Pokhara in Year 2018 A.D

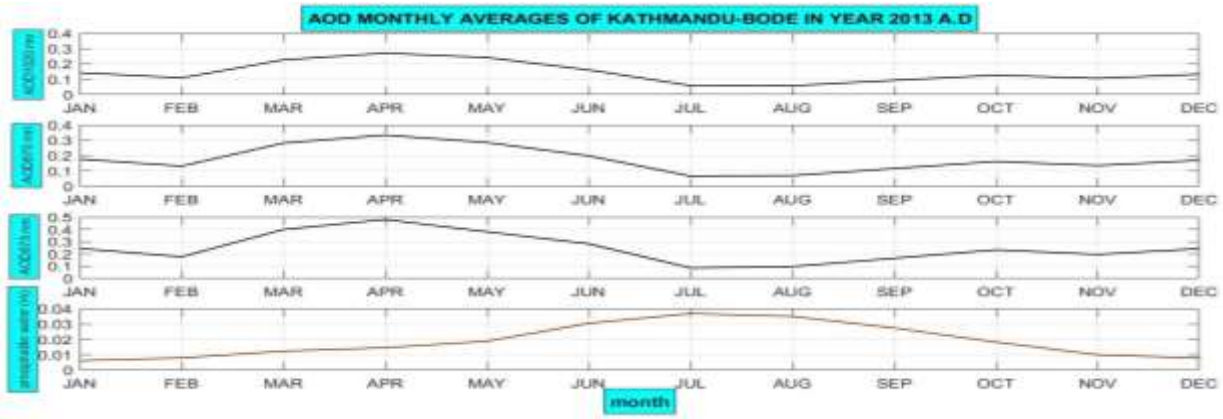

Fig. 4: The first three panel shows the variation of AOD with respect to three different wavelength i.e. 1020nm, 870nm and 675nm respectively and, the fourth panel shows the variation of AOD to precipitated water of Kathmandu-Bode in Year 2013 A.D.

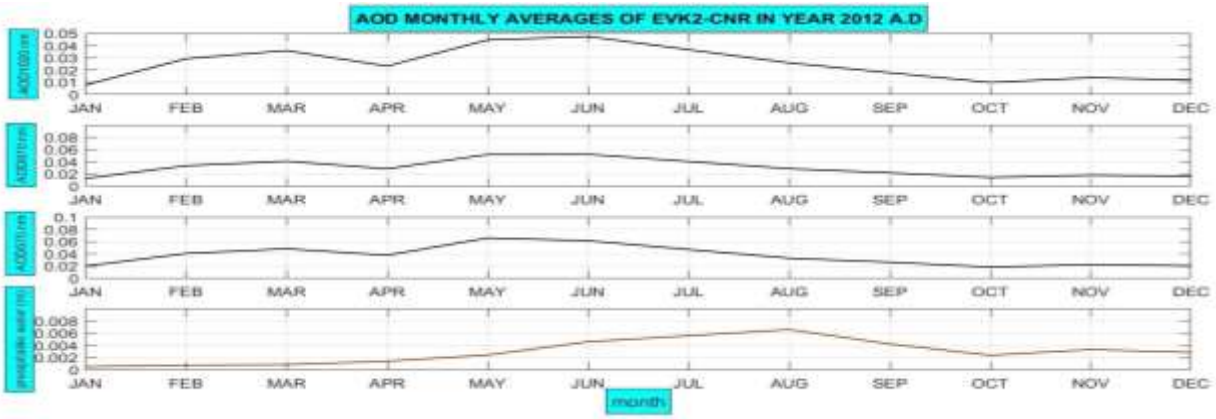

Fig. 5*:* The first three panel shows the variation of AOD with respect to three different wavelength i.e. 1020nm, 870nm and 675nm respectively and, the fourth panel shows the variation of AOD to precipitated water of EVK2-CNR in Year 2012 A.D.

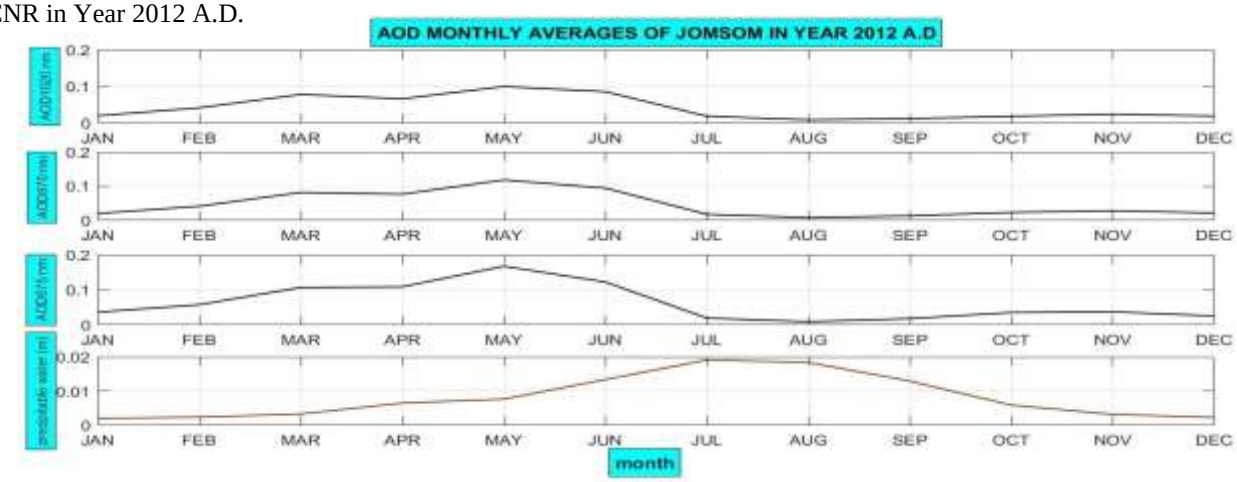

Fig. 6: The first three panel shows the variation of AOD with respect to three different wavelength i.e. 1020nm, 870nm and 675nm respectively and, the fourth panel shows the variation of AOD to precipitated water of Jomsom in Year 2012 A.D.

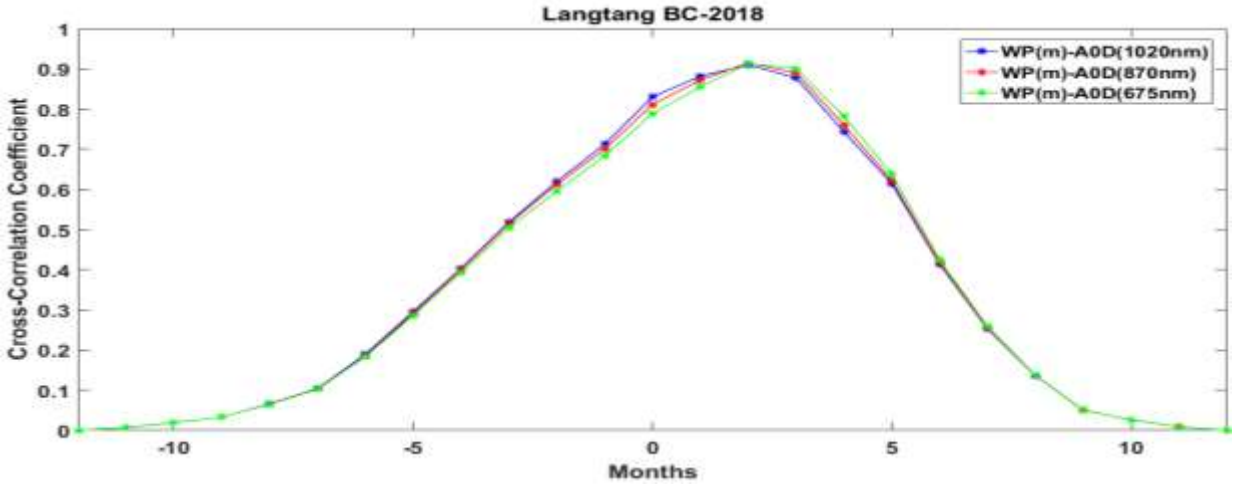

Fig. 7*:* Represents the cross-correlation between Precipitated water and AOD at three different wavelength i.e. 1020nm, 870nm and 675nm of Langtang BC in year 2018 A.D.

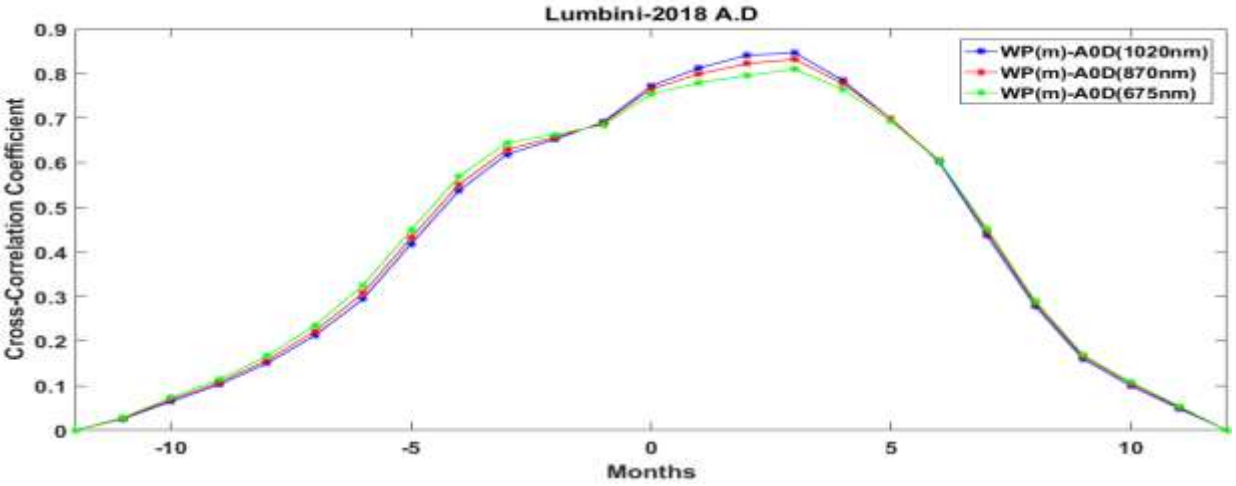

Fig. 8: Represents the cross-correlation between Precipitated water and AOD at three different wavelength i.e. 1020nm, 870nm and 675nm of Lumbini in year 2018 A.D.

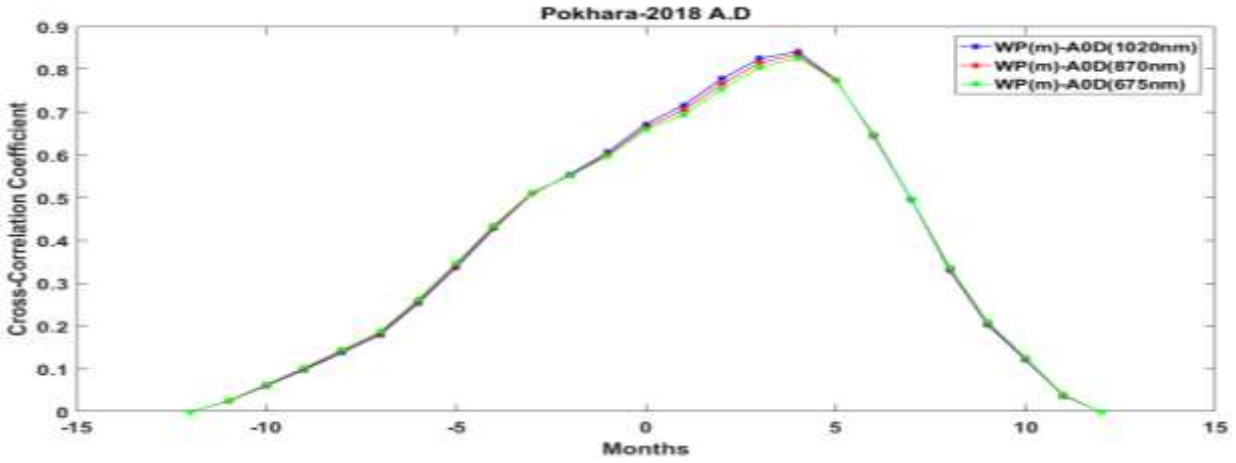

Fig. 9: Represents the cross-correlation between Precipitated water and AOD at three different wavelength i.e. 1020nm, 870nm and 675nm of Pokhara in year 2018 A.D.

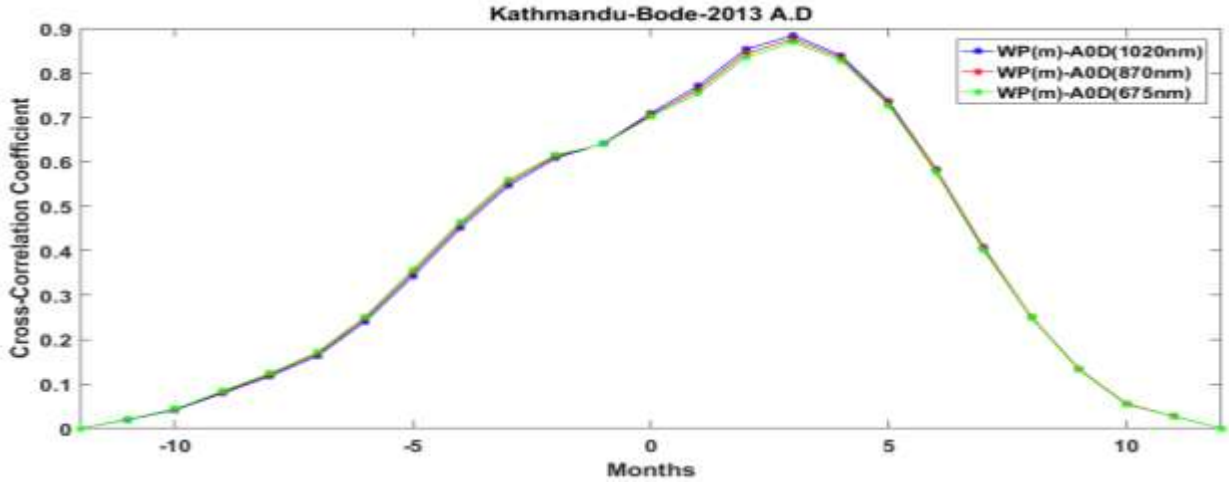

Fig. 10*:* Represents the cross-correlation between Precipitated water and AOD at three different wavelength i.e. 1020nm, 870nm and 675nm of Kathmandu-Bode in year 2013 A.D.

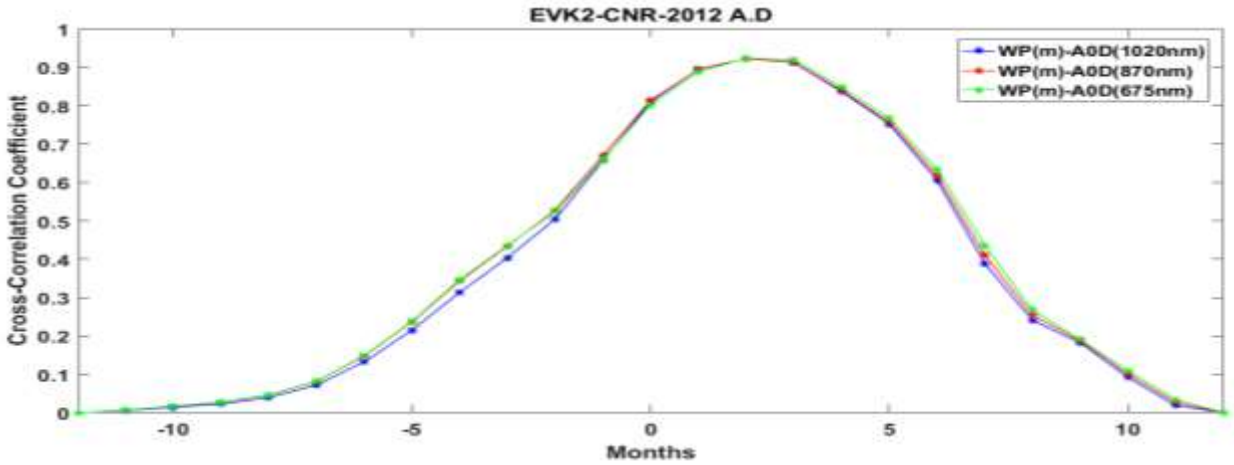

Fig. 11: Represents the cross-correlation between Precipitated water and AOD at three different wavelength i.e. 1020nm, 870nm and 675nm of EVK2-CNR in year 2012 A.D.

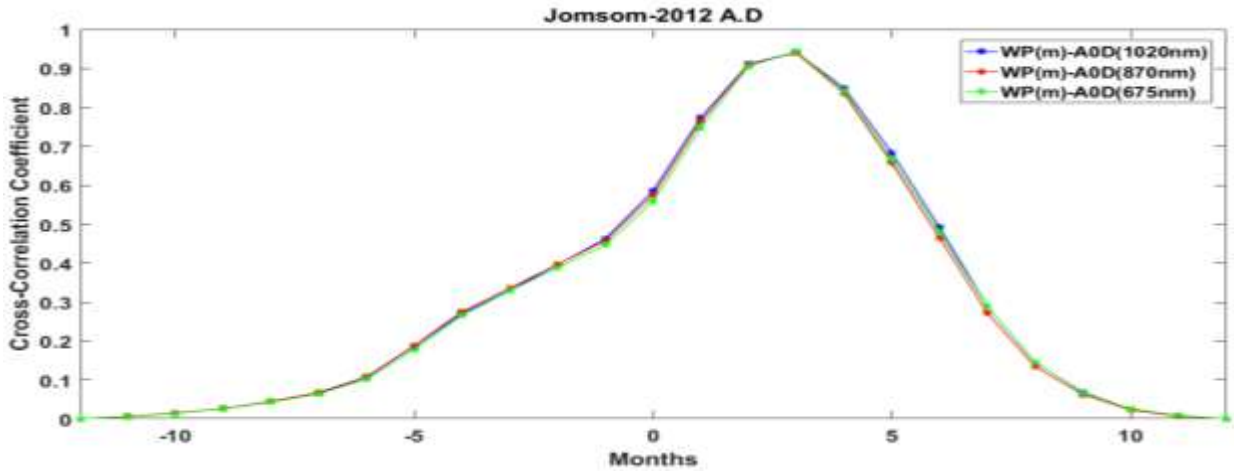

Fig. 12: Represents the cross-correlation between Precipitated water and AOD at three different wavelength i.e. 1020nm, 870nm and 675nm of Jomsom in year 2012 A.D.

Monthly variation of AOD

The monthly variation shows that: AOD was in increasing order from January to February at Langtang, EVK2-CNR, and Jomsom. It was however comparatively less from August to December. This is because, these places are situated in the Himalayan region: in January and February, winter biomass burning plays an important role and the significant portion of the population relies on traditional fuels such as wood, straw, and dung for cooking and heating homes too. These organic fuels deliver a heavy load of particles to the atmosphere [27] because people tend to burn them at relatively cool temperatures; this leads to incomplete combustion also stated by [28]. As winter starts with December, days are less hazy compared to January and February due to which AOD is less in these months compared to January and February. August recorded decreasing AOD: as of August mainly includes wet days of months. September begins with the ending of monsoon, due to which the sky is clear and AOD is reduced. In figure2 and figure3, it was observed that AOD is soaring in January, February, and December. This is the result of traffic and pollution from factories which also contributes to the winter haze in Lumbini and Pokhara [29]. Figure 4 AOD is observed to be increasing in January and December, this is because the maximum of brick kilns are situated in Kathmandu-Bode [30]. It is also in these months, the meteorological parameters showed significant fluctuations. The relative humidity was normally greater than 97%, as shown by[31]. A similar pattern is followed in Lumbini. Figure1, figure2, figure3, and figure4 AOD are in increasing order from February to April due to land clearing and agricultural fires in various regions of Nepal[6]. In figure 1-6, AOD was observed to be decreasing in July due to wet days of summer [32]. Nepal's summer season comprises both wet and dry days, while in wet days aerosol is detached due to precipitation and in dry days the maximum number of aerosol goes to the atmosphere due to dry wind and pollution caused by various human activities[33]. Sometimes, this maximum amount of aerosol with some amount of water molecules form a group of large clouds resulting in catastrophic rainfall. In Figure5: AOD is not significantly less in July, because EVK2-CNR does not follow the trend of wet days or only a few amounts of rain may occur during this time. The AOD can be seen increasing in Figure1, Figure2, Figure4, Figure5, and Figure6 in May and June because these are the dry months of summer as similar result of [34] with no significant rainfall and most of the pollutants are drifted to the atmosphere by this dry wind. However, in figure3 AOD can be seen to be decreased in June because Pokhara is the only city all over Nepal where the monsoon starts early and it lasts for long, so in Pokhara, June comes into the wet days of summer.

Seasonal variation

Figure13-15 represents the contour plot of seasonal variation of AOD at 1640nm of Pokhara, Kyanjin_Gompa, and Lumbini in the year of 2018, respectively. In the contour plot, Season was placed in the y-axis, an hour was in the x-axis and AOD was placed in the z-axis. It has been noticed that AOD is increasing in winter and is maximum in spring and drastically decreasing in summer, however, it was more in autumn compared to summer in the case of Pokhara. But AOD is minimum in autumn than in summer for Kyanjin_Gompa and Lumbini. These three-station i.e. Pokhara, Kyanjin_Gompa, and Lumbini were taken under consideration for seasonal variation which encompasses all three geographical regions of Nepal. Lumbini lies in the Terai region, Pokhara lies in the Hilly region and Kyanjin_Gompa lies Himalayan region. From the above figures, it was observed that Lumbini has the aerosol of the highest optical depth compared to Pokhara and Kyanjin_Gompa also, Pokhara has less AOD than Lumbini but more than Kyanjin_Gompa.

Seasonal variation graphs of AOD concludes that: AOD was found to be increasing in winter and was

maximum in spring and drastically decreases in summer and was minimum in autumn, however, it was more in autumn compared to summer in case of Pokhara. It is due to, increment in heating needs, vehicle traffic, and industry which contributes to winter haze in cities like Pokhara and Lumbini. Pokhara also lies in such a region of Nepal where a significant amount of biomass burning, and downwind of the Indo-Gangetic plains contributes to haze during winter and spring [6]. Bricks production in winter also helps in the ejection of aerosol to the atmosphere in Lumbini and Kathmandu-Bode. In the case of Kyanjin_Gompa, most of the population are dependent on traditional fuels such as woods, straw, dried dung for cooking and also for heating purpose in winter. These organic fuels contribute to a heavy load of particles in the atmosphere. Also high Himalayas is dominated by higher concentrations during winter and spring (pre-monsoon), minimal concentrations during the summer wet monsoon season, and increasing levels during the autumn (post-monsoon) [35]. Spring season begins with occasional shower and pollution had contributed to spring haze, as in 2018 A.D Nepal is considered as one of the most polluted countries added with the most degraded air quality. So in spring, AOD was found to be maximum in all three stations. Vegetation fires peak in the Himalayan region in April [6], which has a large impact on all three sites. It was also observed that in summer, AOD of Pokhara goes to a minimum because most of the month of summer is wet days of monsoon and due to heavy rainfall maximum amount of aerosol flushes out. But in the case of Lumbini and Kyanjin_Gompa summer includes both wet and dry days of monsoon due to which only a minimum amount of aerosol gets detach while in the wet days. Autumn: the season starts with the ending of monsoon resulting in lesser AOD compared to other seasons in the context of Nepal [22]. Autumn is also considered as the best season for outdoor activities like trekking, jungle safari, rafting, etc. as you can enjoy lots of green and blue sky

Pokhara significantly has lesser AOD than Lumbini but more than Kyanjin_Gompa. In summary, Kyanjin_Gompa does have relatively pristine environments occasionally disturbed by pollution episodes. Pokhara and Lumbini, however, are seriously affected by human activities. AOD at Pokhara and Lumbini is much higher than the Kyanjin_Gompa in each month similar to the result of [6].

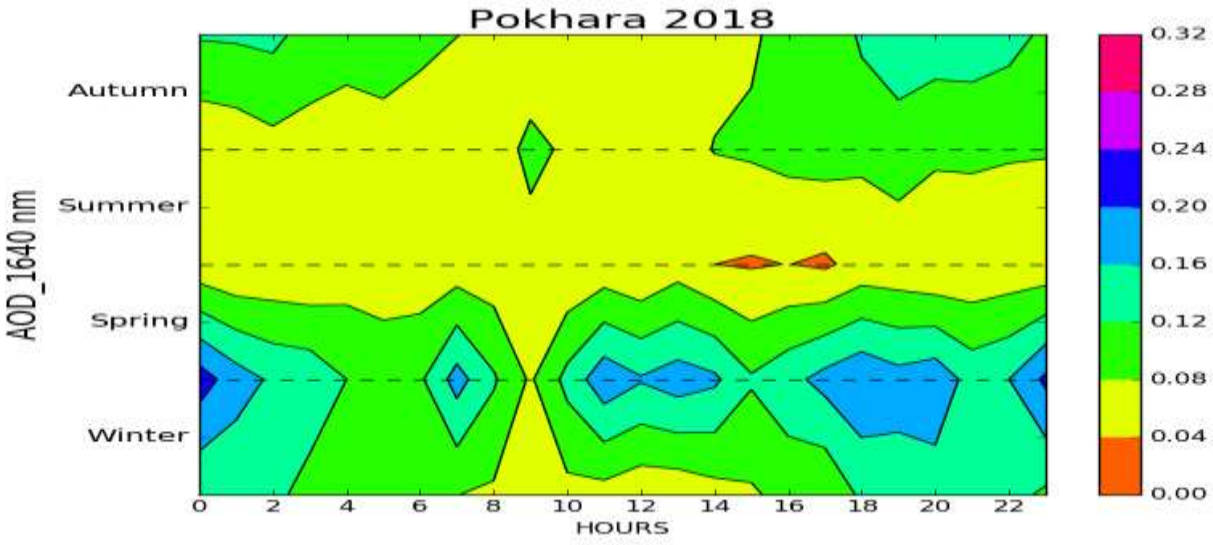

Fig. 13: Shows the Seasonal variation of AOD at 1640nm wavelength of Pokhara in year 2018.

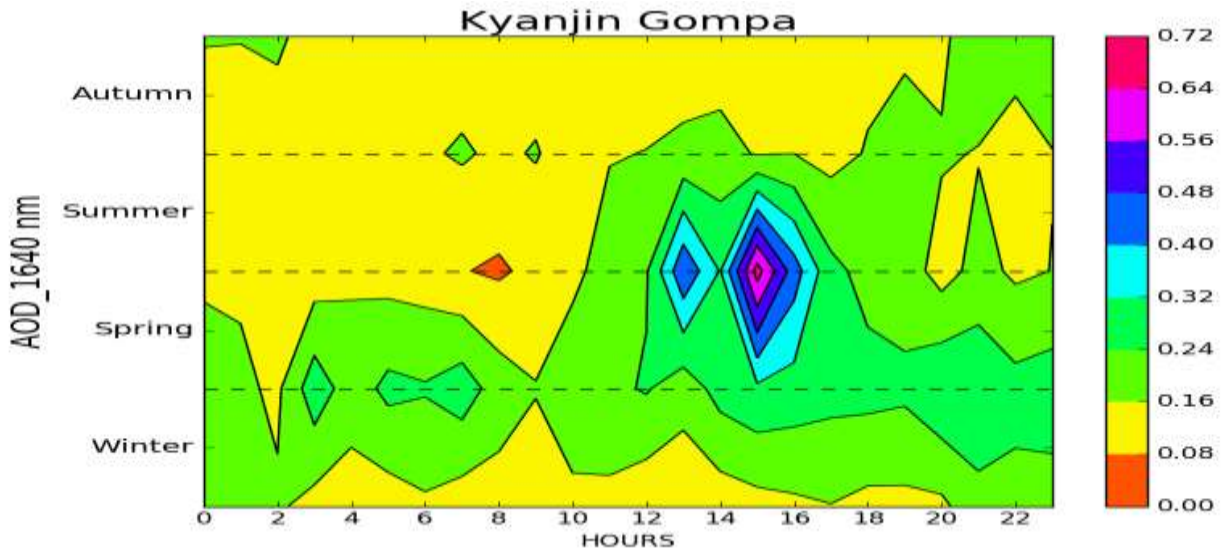

Fig. 14: Shows the Seasonal variation of AOD at 1640nm wavelength of Kyanjin_Gompa in year 2018 A.D.

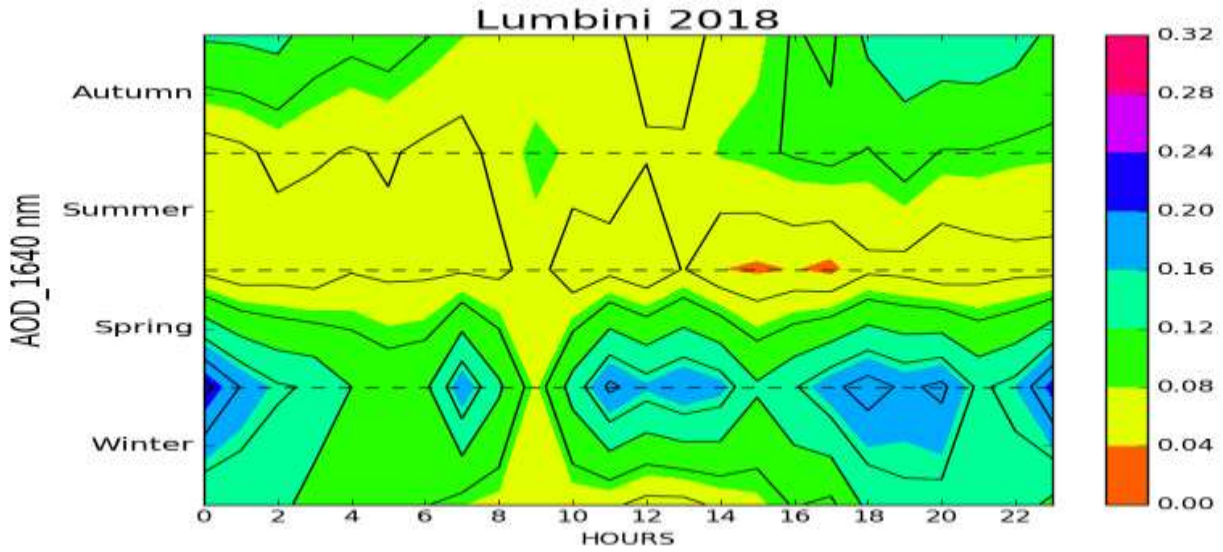

Fig. 15: Shows the Seasonal variation of AOD at 1640nm wavelength of Lumbini in year 2018 A.D**.**

4. Conclusion and general remarks

We have investigated the aerosol optical properties at various tourist places in Nepal concerning wavelength and precipitated water. Besides that, we have also observed the monthly and seasonal variation of AOD. We conclude our results as follows :

- An inverse relationship between wavelength and AOD was established because of Angstrom Exponent. Angstrom exponent is inversely related to the standard size of the particles within the aerosol: the smaller the particles, the larger the exponent [36]. Thus, it is a useful quantity to assess the particle size of atmospheric aerosols or clouds, and the wavelength dependencies of the aerosol/cloud optical properties[37]. The angstrom exponent

states that the optical thickness of an aerosol depends on the wavelength of light, as mentioned by [38].

- From the above result, it was clear that aerosol plays an important role in precipitation, or also we can say that they are inversely related to each other in July and August as these months include a massive rainfall in case of Nepal. This result is like the result produced by [7] where they suggest that changes in precipitation were likely due to aerosol interactions. The amount of aerosol plays an important role in precipitation. If there are a large number of aerosols, then water molecules will have more options for condensation because of which small clouds are formed with no or very few precipitations as water droplets in the cloud need to reach in critical size for a downpour. However, if there are fewer aerosols in our atmosphere then more water molecules get attached to those few aerosol-forming large as well as grey clouds resulting in rainfall, hence the maximum number of aerosol flush out due to rainfall because precipitation is directly correlated with AOD given by the study of [26].
- From above result it was inferred that, maximum increase in AOD is in April due to vegetation fire which helps to contribute in spring haze, in different regions of Nepal. Adding up, acceleration of AOD in January, February and December is the outcome of the bio-mass burning, wood and dung for cooking, heating needs in the stations like Kyanjin_Gompa, Langtang BC, EVK2-CNR, Jomsom which is situated in Himalayan region. Likewise, bricks kiln, vehicle traffic, heating needs, pollution from factories are main source of AOD in the stations like Kathmandu-Bode, Pokhara and Lumbini.
- From the above result i.e. the reduction of AOD in July in all the station except EVK2-CNR concludes that, all the other stations except EVK2-CNR follow the trend of wet days of summer while wet days of summer include precipitation and due to which aerosol get detached from atmosphere. However, EVK2-CNR do not follow the trend of wet days. Also, all the stations except Pokhara shows the acceleration of AOD in the month of May and June because these two are considered as a dry months of summer with no significant rainfall and most of the pollutant are drifted up by dry wind. However, Pokhara is the only city in Nepal where monsoon starts early and last for long so June belongs to wet days of summer in case of Pokhara.

In summary, Pokhara shows less AOD than Lumbini but more than Kyanjin_Gompa. .Kyanjin_Gompa shows relatively pristine environments occasionally disturbed by pollution episodes. Pokhara and Lumbini, however, are seriously affected by human activities. AOD at Pokhara and Lumbini was much higher than the Kyanjin_Gompa in each month as the result of [6]. The result presented in this work may help to enhance more knowledge about the Aerosol Optical Properties of different tourist places as well as all the three geographical regions of Nepal. Aerosol monthly, seasonal variation at different stations as well as geographical regions are elucidated based on the objective phenomenon of precipitation, wavelengths, and source emission variations. To improve knowledge about the study of its effect and control measure, more direct evidence, such as chemical sampling at different atmospheric layers, micro-pulse LIDAR observations from the surface, or LIDAR remote-sensing measurements have to be used in future studies.

Acknowledgment

We would like to thank Gian Paolo Gobbi of the institute of atmospheric science and climate (CNR-ISAC) for his valuable advice and assistance during the data collection and also would like to thank Brent Holben and Arnico Panday, the co-investigator and principle investigator of various station of Aerosol in Nepal for providing reliable

data for observation. We would also like to extend our thanks to the Department of Physics, St. Xavier College for the support. The authors also gratefully acknowledge the efforts made by the AERONET team/site[39] PIs and operators including at Langtang BC, Pokhara, Lumbini, Kathmandu-bode, EVK2-CNR, Kyanjin_Gompa, and Jomsom.

References

[1] S. Tariq et al., Variability of size distribution , refractive index and assymetric parameter of aerosols over lahore derived from AERONET. 24 (2013) 137–139.

[2] R. R. Kommalapati and K. T. Valsaraj Atmospheric aerosols and their importance, ACS Symp. Ser. 1005 (2009) 1–10. https://pubs.acs.org/doi/10.1021/bk-2009-1005.ch001

[3] D. M. Giles *et al.*, An analysis of AERONET aerosol absorption properties and classifications representative of aerosol source regions, J. Geophys. Res. Atmos. 117 (2012). https://doi.org/10.1029/2012JD018127

[4] Aerosols: Tiny Particles, Big Impact. https://earthobservatory.nasa.gov/features/Aerosols

[5] T.Takemura et al., Single-scattering albedo and radiative forcing of various aerosol species with a global three-dimensional model, J. Clim. 15 (2002) 333–352. https://doi.org/10.1175/1520-0442(2002)015<0333:SSAARF>2.0.CO;2

[6] C. Xu *et al.*, Similarities and differences of aerosol optical properties between southern and northern sides of the Himalayas, Atmos. Chem. Phys. 14 (2014) 3133–314. https://doi.org/10.5194/acp-14-3133-2014

[7] G. Thompson and T. Eidhammer, A Study of Aerosol Impacts on Clouds and Precipitation Development in a Large Winter Cyclone, J. Atmos. Sci. 71 (2014) 3636–3658. http://journals.ametsoc.org/doi/abs/10.1175/JAS-D-13-0305.1

[8] B. Qi *et al.*, Seasonal Variation of Aerosol Optical Properties in an Urban Site of the Yangtze Delta Region of China. (2016) 2884–2896. https://doi.org/10.4209/aaqr.2015.05.0350

[9] V. Martins et al., Deposition of aerosol particles from a subway microenvironment in the human respiratory tract, J. Aerosol Sci. 90 (2015) 103–113. http://dx.doi.org/10.1016/j.jaerosci.2015.08.008

[10] M. A. Alghoul et al., Impact of aerosol optical depth on solar radiation budget, Proc. 3rd WSEAS Int. Conf. Energy Planning, Energy Saving, Environ. Educ. EPESE '09, Renew. Energy Sources, RES '09, Waste Manag. WWAI 09(2009)386–393. https://www.researchgate.net/publication/316824656_Impact_of_Aerosol_Optical_Depth_on_Solar_Radiation_Budget

[11] .https://aeronet.gsfc.nasa.gov/cgi-bin/webtool_aod_v3.

[12] A. Smirnov et al., Cloud-screening and quality control algorithms for the AERONET database RID C-2121-2009 RID A-8235-2009, Remote Sens. Environ.73 (2000) 337–349. https://doi.org/10.1016/S0034-4257(00)00109-7

[13] https://aeronet.gsfc.nasa.gov/new_web/photo_db_v3/Langtang_BC.html.

[14] https://aeronet.gsfc.nasa.gov/new_web/photo_db/Lumbini.html

[15] https://aeronet.gsfc.nasa.gov/new_web/photo_db/Pokhara.html

[16] https://aeronet.gsfc.nasa.gov/new_web/photo_db/Kathmandu-Bode.html

[17] https://aeronet.gsfc.nasa.gov/new_web/photo_db/EVK2-CNR.html

[18] https://aeronet.gsfc.nasa.gov/new_web/photo_db/Jomsom.html

[19] https://aeronet.gsfc.nasa.gov/new_web/photo_db/Kyanjin_Gompa.html

[20] https://www.investopedia.com/terms/c/crosscorrelation.asp

[21] B. Adhikari et al., Impacts on Cosmic-Ray Intensity Observed During Geomagnetic Disturbances, Sol. Phys. 292 (2017). .http://dx.doi.org/10.1007/s11207-017-1183-3

[22] S. Marcq et al., Aerosol optical properties and radiative forcing in the high Himalaya based on measurements at the Nepal Climate Observatory-Pyramid site (5079 m a.s.l.), Atmos. Chem. Phys.10 (2010) 5859–5872. https://doi.org/10.5194/acp-10-58592010.

[23] contour map (article)|Khan Academy. https://www.khanacademy.org/math/multivariable-calculus/thinking-about-multivariable-function/ways-to-represent-multivariable-functions/a/contour-maps.

[24] G. L. Schuster et al., Angstrom exponent and

bimodal aerosol size distributions Angstrom exponent and bimodal aerosol size distributions. (2016). https://doi.org/10.1029/2005JD006328

[25] N. Aeronautics, Atmospheric Aerosols. (1996). https://dx.doi.org/10.1002/9783527630134.ch12

[26] S. M. Kreidenweis et al., 100 Years of Progress in Cloud Physics, Aerosols, and Aerosol Chemistry Research, Meteorol. Monogr. 59 (2019) 11.1-11.72. https://doi.org/10.1175/AMSMONOGRAPHS-D-18-0024.1

[27] S. Oeder et al., Particulate matter from both heavy fuel oil and diesel fuel shipping emissions show strong biological effects on human lung cells at realistic and comparable in vitro exposure conditions, PLoS One. 10 (2015) 1–17. https://doi.org/*10*.1371/journal.pone.0126536

[28] M. Zhang et al., Aerosol optical properties of a haze episode in Wuhan based on ground-based and satellite observations, Atmosphere (Basel). 5 (2014) 699–719. https://doi.org/10.3390/atmos5040699

[29] D. R. Gautam, Air Pollution: Its Causes and Consequences With Reference To Kathmandu Metropolitan City, Third Pole J. Geogr. Educ. 8 (2014) 27–33. https://doi.org/10.3126/ttp.v8i0.11509

[30] M. Zhong *et al.*, Nepal Ambient Monitoring and Source Testing Experiment (NAMaSTE): Emissions of particulate matter and sulfur dioxide from vehicles and brick kilns and their impacts on air quality in the Kathmandu Valley, Nepal, Atmos. Chem. Phys. Discuss. (2018) 1–34. https://doi.org/10.5194/acp-2018-599

[31] N. P. Sharma et al., Study on Aerosol Optical Depth in Winter and Summer Season in Bhaktapur, J. Inst. Eng. 8 (1970) 269–276. https://doi.org/10.3126/jie.v8i1-2.5122.

[32] L. Zhang et al., Multi-time scale analysis of regional aerosol optical depth changes in national-level urban agglomerations in China using MODIS collection 6.1 datasets from 2001 to 2017, Remote Sens.11 (2019) 201. https://doi.org/10.3390/rs11020201.

[33] B. C. Bhattarai et al., Aerosol optical depth over the nepalese cryosphere derived from an empirical model, Front. Earth Sci.7 (2019) 1–17. https://doi.org/10.3389/feart.2019.00178.

[34] A. Deroubaix et al., Interactions of atmospheric gases and aerosols with the monsoon dynamics over the Sudano-Guinean region during AMMA, Atmos. Chem. Phys.18 (2018) 445–465. .https://doi.org/10.5194/acp-18-445-2018

[35] P. Bonasoni et al., Atmospheric Pollution in the Hindu Kush–Himalaya Region, Mt. Res. Dev. 32 (2012) 468–479. https://doi.org/10.1659/MRD-JOURNAL-D-12-00066.1

[36] K. Soni et al., Wavelength dependence of the aerosol Angstrom exponent and its implications over Delhi, India, Aerosol Sci. Technol. 45 (2011) 1488–1498. https://doi.org/10.1080/02786826.2011.601774

[37] H. Jethva and O. Torres, Satellite-based evidence of wavelength-dependent aerosol absorption in biomass burning smoke inferred from Ozone Monitoring Instrument, Atmos. Chem. Phys.11 (2011) 10541–10551. https://doi.org/10.5194/acp-11-10541-2011.

[38] D. G. Kaskaoutis and H. D. Kambezidis, Investigation into the wavelength dependence of the aerosol optical depth in the Athens area, Q. J. R. Meteorol. Soc. 32 (2006) 2217–2234. https://doi.org/10.1256/qj.05.183

[39] https://aeronet.gsfc.nasa.gov/cgi-bin/bamgomas_maps_index_v3